

## Experimental Observation of Speckle Instability in Kerr Random Media

U. Bortolozzo,<sup>1</sup> S. Residori,<sup>1</sup> and P. Sebbah<sup>2,\*</sup>

<sup>1</sup>*INLN, Université de Nice Sophia-Antipolis, CNRS, 1361 route des Lucioles 06560 Valbonne, France*

<sup>2</sup>*LPMC, Université de Nice Sophia-Antipolis, CNRS, Parc Valrose 06108 Nice Cedex 2, France*

(Received 16 March 2010; revised manuscript received 27 January 2011; published 11 March 2011)

In a disordered nonlinear medium the transmitted speckle pattern was predicted to become unstable as a result of the positive feedback between intensity fluctuations and local variations of the refractive index. We show experimental evidence of speckle instability for light transversally scattered in a liquid crystal cell, where a two-dimensional controlled disorder is imprinted by suitable illumination of a photoconductive wall and nonlinearity is obtained through optical reorientation of the liquid crystal molecules. The speckle pattern spontaneously oscillates at discrete frequencies above a critical threshold, whose dependence on the scattering mean free path confirms the crucial role of disorder in the feedback process.

DOI: [10.1103/PhysRevLett.106.103903](https://doi.org/10.1103/PhysRevLett.106.103903)

PACS numbers: 42.25.Dd, 42.55.Zz

In a disordered medium, the transmitted intensity measured at a point results from the interference of light incoming from all possible scattering trajectories inside the medium. These constructive and destructive interferences give rise to intensity fluctuations [1]. The resulting speckle pattern is a fingerprint of the medium traversed by the wave and is highly sensitive, for instance, to scatterer displacements within the medium. This property has been applied to speckle imaging [2] or diffuse wave spectroscopy [3]. Sensitivity of the speckle pattern to frequency or polarization shift of the incident beam has been used in recent decades to explore speckle fluctuations and correlations in mesoscopic samples [4]. But changes in speckle pattern can also be achieved by intensity variation of the input beam when considering a nonlinear (NL) scattering medium with a Kerr-type nonlinearity. Local intensity fluctuations induce local refractive-index changes, which in turn modify the optical trajectories. The intensity fluctuations are redistributed within the sample, resulting in a new transmitted speckle pattern. Under certain conditions, this feedback mechanism was predicted to become unstable leading to spontaneous dynamics of the speckle pattern [5–9]. The instability threshold  $p = \langle n_2 I \rangle^2 \times (L/\ell)^3 > 1$  was calculated, which is reached for any value of the NL correction  $n_2 I$  to the refractive index, as long as the mean free path  $\ell$  is small enough,  $L$  being the system size. Therefore, speckle instabilities differ from common unstable regimes observed in NL optics, since here the feedback is provided by multiple scattering. To date, experimental observation of speckle instability has never been reported.

In this Letter, we report the first experimental evidence of speckle instability. A liquid crystal (LC) cell serves simultaneously as the scattering and Kerr NL medium. A two-dimensional (2D) computer-generated image of random scatterers is projected on a photoconductive wall of the cell, generating a controlled 2D random distribution of the refractive-index within the LC layer. A probe laser

beam is transversally scattered while inducing a NL Kerr-reorientation of the LC molecules. Speckle pattern spontaneous oscillations are observed. Instability threshold is identified and found to be dependent on scattering mean free path, in agreement with the theory. Periodic oscillations are observed at threshold, followed by a frequency cascade at higher probe intensity, in contrast to the chaotic regime with continuous spectrum predicted by theory. Based on NL energy transfer and natural gain selection, a simple model is here proposed to explain the dynamics and the frequency selection. Light scattering in random and NL media has attracted considerable attention recently with, for instance, the exploration of the impact of a nonlinearity on Anderson localization [10,11] or the role of disorder on solitons [12]. Beyond the observation of this new physical phenomenon, our experimental study is among the very first [13] to explore the dynamic interplay between nonlinearity and multiple scattering. These questions have attracted recently strong interest in a broad scope of fields, including Bose-Einstein condensation.

The experimental setup is sketched in Fig. 1. The  $20 \times 30$  mm LC light valve is composed of a  $L = 55 \mu\text{m}$ -thick LC film in the nematic phase and a 1 mm-thick  $\text{Bi}_{12}\text{SiO}_{20}$  (BSO) photoconductive substrate, sandwiched between two transparent indium-tin-oxide electrodes [14]. A random pattern (here a random collection of dark disks in a white background, as shown in top-right inset of Fig. 1) is computer generated and transmitted to a  $36.9 \text{ mm} \times 27.6 \text{ mm}$  spatial-light modulator (SLM), spatial resolution  $1024 \times 768$  pixels, which serves as a 2D random mask. The local voltage applied across the LC film decreases where light impinges on the BSO crystal, inducing local LC reorientation. A given light intensity distribution is therefore converted into a corresponding distribution of molecular orientation. As a result of LC birefringence, a 2D refractive-index distribution invariant along the longitudinal direction,  $n(x, y)$ , is formed within the LC film, which reproduces the initial random pattern. Because the

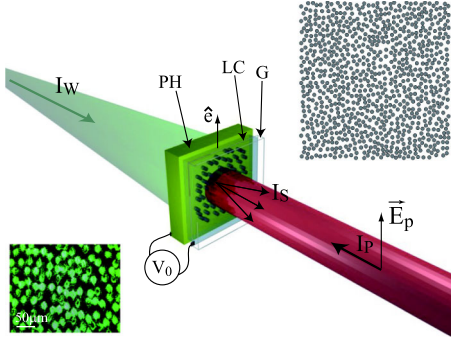


FIG. 1 (color online). Sketch of experimental setup. The computer-generated disorder configuration (top-right inset) is projected onto the photoconductive wall (PH) of the LC light valve, using a green laser beam ( $I_W$ ) and a spatial-light modulator (not shown). The near-field image of the random distribution of refractive index generated within the LC is shown in the bottom-left inset. The speckle pattern ( $I_S$ ) results from transverse scattering of the beam ( $I_S$ ) as it propagates back and forth through the LC film after reflection at the interface with PH of the red probe beam ( $I_P$ ). The probe field  $\vec{E}_p$  is parallel to the LC nematic director  $\hat{e}$  (extraordinary polarization) determined by surface anchoring. The nonlinearity is provided by the molecular reorientation of the liquid crystal under the action of the red laser ( $I_P$ ). (G = glass cover.)

BSO crystal is sensitive to the blue-green region of the spectrum, a cw diode-pumped solid state laser at 532 nm is used as the writing beam with an intensity of 2 mW/cm<sup>2</sup>. The refractive-index distribution is monitored by a 8-bit CCD camera and is shown in the bottom-left inset of Fig. 1. The geometrical characteristics of the LC scattering medium are fully controlled by adjusting the filling fraction  $\phi$ , the diameter  $D$  and positions of the scatterers. By shrinking the image on the computer screen, the actual scatterer diameter can be varied from  $D = 100 \mu\text{m}$  to  $10 \mu\text{m}$ , leaving  $\phi$  constant. The refractive index of the scatterers,  $n_s$ , varies between  $n_o = 1.52$  and  $n_e = 1.75$ , according to the 8-bit coded gray level of the SLM mask, where  $n_o$  and  $n_e$  are, respectively, the ordinary and the extraordinary index of the LC. In the following, we choose  $\phi = 40\%$ ,  $D = 50$ , or  $20 \mu\text{m}$  and  $n_s = n_e = 1.75$  while  $n = n_o$  for the surrounding LC.

A linearly polarized HeNe laser (632.8 nm wavelength, 5 mW power, spot-size  $w_0 = 380 \mu\text{m}$ ) serves as the probe beam. Its polarization is parallel to the LC nematic director. The probe beam is transversally scattered as it propagates along the LC layer, which behaves as a random array of weakly coupled waveguides [10,11] and is backreflected at the LC/BSO interface with a total reflectivity of 22%. This confirms that propagation remains in the paraxial approximation limit and allows us to estimate the mean free path in the transverse direction. Indeed in this limit, the wave equation reduces to a Schrödinger equation where time is replaced by longitudinal coordinate  $z$  to describe a particle moving in a 2D potential

$-V(x, y) = -k^2[n^2(x, y) - n_0^2]$ . It writes  $2ikn_0 \frac{\partial A}{\partial z} = (\nabla_{xy}^2 + V(x, y))A$  where  $A(x, y, z) \exp(-ikn_0 z)$  is the wave field and  $n_0$  is the effective refractive index defined by  $n_0 = S^{-1} \int_S n^2(x, y) dx dy$  [15]. When considering transverse scattering, the relevant wave vector is no longer  $k = \omega/c$  but rather the transverse wave vector  $k_{\perp} = \omega/v$ , with  $c/v = k_{\perp}/k \approx 2 \times 10^{-3}$  in our case. Because the ratio  $k/k_{\perp}$  can be larger than 1, the product  $k_{\perp} \ell \ll k\ell$ , making transverse Anderson localization of light possible in finite-sized random systems even for small index contrast [10,11,15]. In our system, a crude estimate of the mean free path from Mie theory (infinite cylinders with index  $n_e$  in a matrix  $n_o$ ) and single scattering approximation yields  $\ell \approx 100 \mu\text{m}$  (respectively  $\ell \approx 40 \mu\text{m}$ ) at 632.8 nm for  $D = 50 \mu\text{m}$  (respectively  $D = 20 \mu\text{m}$ ). The localization length in 2D is given by  $\xi \approx \ell \exp(\pi k_{\perp} \ell / 2)$ . As it propagates freely along the longitudinal direction, the beam extends transversally, experiencing successively a ballistic regime ( $t < \tau_0 = \ell/v$ ), a subdiffusive multiple-scattering regime ( $\tau_0 < t < T_{\text{loc}}$ ) [16], and a crossover to localization ( $t > T_{\text{loc}} = 2\xi^2/v\ell$ ). To identify the regime reached within the round-trip ballistic time  $t_b = 2L/c$  spent in the LC cell, we estimate  $t_b/\tau_0 = (2L/\ell)(k/k_{\perp}) \approx 5 \times 10^2$  (respectively  $10^3$ ), and  $t_b/T_{\text{loc}} = t_b/\tau_0 \times \exp(-\pi k_{\perp} \ell) \approx 0.9$  (respectively 80). Although based on a rough estimate of the mean free path, these calculations demonstrate that the multiple-scattering regime is well established, even though the localization regime may not be yet fully attained.

During its round-trip propagation in the cell, the extraordinary-polarized probe beam experiences NL scattering as its electric field changes molecule orientation. Laser-induced LC reorientation translates into an intensity-dependent refractive index and provides a very large optical Kerr nonlinearity, with a nonlinear coefficient  $n_2$  orders of magnitude larger than of commonly used media [17]. Its noninstantaneous dynamics can be described by a Debye relaxation equation,  $\tau_{\text{NL}} \partial_t n = -(n - n_c) + l_D^2 \nabla_{\perp}^2 n + n_2 I$ , where  $\tau_{\text{NL}} = \gamma L^2 / \pi^2 K$ , with  $\gamma$  the LC rotational viscosity and  $K$  the elastic constant corresponding to deformation of the LC alignment. In our case,  $\tau_{\text{NL}} \approx 410$  ms, for typical values  $\gamma = 0.02 \text{ Pa} \cdot \text{s}$ ,  $K = 15 \text{ pN}$  [18,19]. The same time constant,  $\approx 400$  ms, has been independently found by measuring directly the response time of the optical reorientational effect. This is a rather slow nonlinearity. The scattering system and the speckle can therefore be safely considered stationary during beam propagation back and forth across the LC film and the parabolic equation remains valid. Finally, the electric coherence length in the LC,  $l_D$ , is of a few microns in our case and is negligible compared to the size of our scatterers, simplifying the right-hand side of the relaxation equation.

The back-reflected far-field speckle pattern is imaged onto a second CCD camera and is shown in Fig. 2. Surprisingly, the speckle pattern is not static: we observe with a naked eye a temporal modulation of each speckle

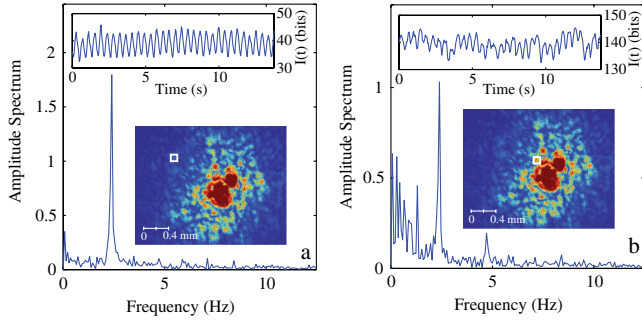


FIG. 2 (color online). Temporal modulation of speckle intensity and corresponding power spectrum within an area encompassing a single speckle spot (delineated by the white square shown in the speckle pattern CCD image). Time-averaged intensity in this area is (a)  $\langle I(t) \rangle = 40$  bits and (b)  $\langle I(t) \rangle = 140$  bits.

spot (as shown in the video [20]). These oscillations are not observed for ordinary polarized light and therefore cannot be attributed to thermal fluctuations. We analyze the speckle oscillations by monitoring over time the modulated intensity, spatially averaged over a small area restricted to a single speckle spot. The temporal oscillations and the corresponding amplitude spectrum are shown in Fig. 2 for two speckle spots with different time-averaged intensity. The low intensity speckle spot shows a single peak at  $f_0 = 2.39$  Hz [Fig. 2(a)]. We find with good agreement  $f_0 \approx 1/\tau_{NL}$ . The speckle instability dynamics is therefore solely driven by the slow response time of the reorientational Kerr nonlinearity. This is another reason why it cannot be related to thermal instabilities since thermal fluctuations are expected to be faster than molecular orientation of the LC (of the order of  $100 \mu\text{s}$  [19]). Besides, given that the intensity used is relatively small and given the small absorption coefficient of pure LC [19], we can safely neglect thermal heating due to laser illumination. Thermal convection can also be excluded because convective patterns in LC have a typical length scale of a few microns [21]; therefore, they would produce a much larger scattering of the probe beam independent of polarization, which is not the case here.

Higher intensity speckle spots show several spectral peaks at  $f_0/2$ ,  $f_0/4$  and also at  $2f_0$ , as in Fig. 2(b). This is further investigated by measuring the oscillation amplitude at these frequencies at speckle positions with similar time-averaged intensity. Despite the broad distributions found (inset of Fig. 3), which is to be expected for the multiple-scattering process is by nature stochastic, the average value of the distribution consistently increases with time-averaged intensity. The amplitude relative to the spectral background vs speckle-spot time-averaged intensity is plotted in Fig. 3 for the four identified oscillation frequencies. Different slopes associated with different threshold are observed for each oscillation frequency. It is remarkable that the intensity dependence of the instability is directly obtained from the speckle pattern nonuniform intensity distribution, as it would be obtained by increasing the input beam intensity.

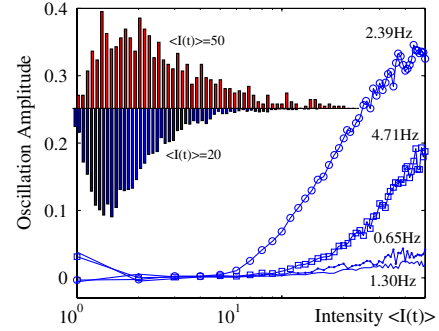


FIG. 3 (color online). Inset: Histograms of oscillation amplitudes measured at positions in the speckle pattern with same time-averaged intensity (top: 20 bits; bottom: 50 bits). Average value of oscillation amplitude plotted vs the time-averaged intensity and for the four frequencies seen in Fig. 2(b).

Next, we investigate the instability threshold dependence with disorder. According to the theoretical predictions the instability threshold is expected to decrease with decreasing mean free path [6,7]. Changing the scatterer dimensions does not affect the oscillation frequency  $f_0$ . We therefore compare the intensity dependence of the peak amplitude at  $f_0$  for different scatterer sizes. Figure 4 shows the measurements for scatterer diameters  $D = 50$  and  $20 \mu\text{m}$ , corresponding, respectively, to  $\ell \approx 100 \mu\text{m}$  and  $\ell \approx 40 \mu\text{m}$ . Although single scattering approximation is known to underestimate the true value of the mean free path, it was shown [22] that the error is in the same direction and of the same order for different scatterer diameters. We can therefore conclude safely that the instability threshold decreases with increasing scattering (decreasing  $\ell$ ). This clearly demonstrates the essential role of disorder in speckle instability and the threshold dependence on the mean free path, as predicted by theory. A theoretical expression of threshold for 2D random systems is not available at this point for direct comparison with experiment.

The temporal modulation of each speckle spot is found to average out when spatial integration is performed, which shows that no phase relation exists from spot to spot. This confirms that our observations are fundamentally different from standard self-phase modulation (SPM) described in the literature for nondisordered media [23]. The uncorrelated oscillations for different speckle spots confirm the nondeterministic nature of the speckle instability, in contrast for instance with the phase-coherent rings observed in SPM.

In contrast to theoretical predictions, we do not observe a chaotic regime at threshold but rather a discrete frequency modulation of the speckle pattern. We propose a simple theory to interpret the frequency selection and frequency cascade in terms of parametric amplification. In a parametric process, a pump beam at  $f_p$  and a probe beam at  $f_m$  interfere to create a grating within the NL material. The pump beam is itself scattered by this grating and nonlinearity-driven energy transfer is achieved from the pump to the probe when  $\Delta f = f_p - f_m \neq 0$ . This



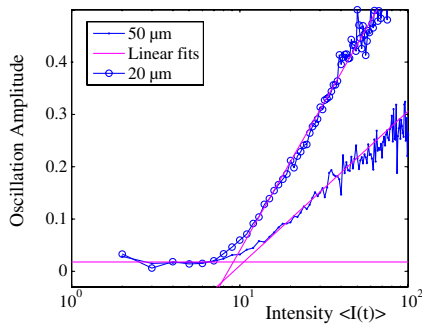


FIG. 4 (color online). Oscillation amplitude at  $f_0 = 2.39$  Hz vs the time-averaged intensity and for two different scatterer diameters  $D = 50$  and  $20 \mu\text{m}$ , corresponding to mean free path  $\ell \approx 100$  and  $40 \mu\text{m}$ , respectively. Solid lines are linear best fits of the data. The threshold, which is materialized by the crossing of the lines, decreases with decreasing  $\ell$ .

transfer of energy via a noninstantaneous Kerr nonlinearity has been interpreted as an amplification process, where the gain reads as  $G(\Delta f) = 2\Delta f\tau_{\text{NL}}[1 + (\Delta f\tau_{\text{NL}})^2]^{-1}$  [24]. The corresponding gain curve is peaked at  $\Delta f = 1/\tau_{\text{NL}}$ . Starting from noise, energy from the pump at  $f_p$  will be preferentially transferred into photons at  $f_m = f_p - 1/\tau_{\text{NL}}$  resulting in the beating of the two beams. In the same way, the spontaneous speckle oscillations observed in our experiment result from the beating between the incident HeNe beam and the nonlinearly generated beam at the maximum of the gain curve, giving rise to a temporal modulation at  $f_0 \approx 1/\tau_{\text{NL}}$ .

In conclusion, we have shown evidence of speckle instabilities in transverse scattering of light in random LC films with a reorientational Kerr effect. The instability is solely attributed to the combination of scattering and Kerr nonlinearity, with uncorrelated oscillations for different speckle spots. It depends on polarization, excluding any thermal effect. The intensity distribution of the speckle allows a direct probing of the intensity dependence of the instability spectrum. A threshold is found which depends on the degree of disorder. This confirms earlier theoretical predictions [6]. The oscillation frequency just above threshold is equal to the inverse of the relaxation time and is interpreted in terms of the beating between the incident beam and a generated light emitted at a frequency equal to the maximum of the gain curve associated with the Kerr effect. Two regimes of speckle instability have been predicted theoretically [9]: a slow NL regime where  $\tau_{\text{NL}} > \tau_D$  driven by the relaxation time of the non linearity, as in the experiment presented here, and a fast NL regime when  $\tau_{\text{NL}} < \tau_D$ . Here,  $\tau_D$  is the time needed by the wave to diffuse transversely through the scattering medium. Therefore, we conjecture that in the fast regime a frequency of oscillation different from  $1/\tau_{\text{NL}}$  should be observed, which will strongly depend on the characteristics of the scattering medium. As in a random laser [25,26], the gain  $G(\Delta f)$  associated with the Kerr nonlinearity will select at threshold an eigenmode at  $f_1$  of the scattering

system, which in turn will beat with the pump, leading to a speckle oscillation at  $f_p - f_1$ . We confirm this prediction numerically. The fast NL regime is, however, out of reach in the present experiment because of the slow reorientational nonlinearity of the LC. A shorter relaxation time could be achieved, for instance, with ferroelectric LC.

This work was supported by the Federation Döblin FR2008 and the French National Research Agency under Grant No. ANR-08-BLAN-0302-01.

\*patrick.sebbah@espci.fr

- [1] J. W. Goodman, *Statistical Optics* (John Wiley, New York, 1985).
- [2] I. Yamaguchi and S. Komatsu, *Opt. Acta* **24**, 705 (1977).
- [3] G. Maret and P. E. Wolf, *Z. Phys. B* **65**, 409 (1987).
- [4] For a recent review, see S. Zhang, Y. D. Lockerman, J. Park, and A. Z. Genack, *J. Opt. A* **11**, 094018 (2009).
- [5] B. Spivak and A. Zyuzin, *Phys. Rev. Lett.* **84**, 1970 (2000).
- [6] S. E. Skipetrov and R. Maynard, *Phys. Rev. Lett.* **85**, 736 (2000).
- [7] S. E. Skipetrov, *Phys. Rev. E* **63**, 056614 (2001).
- [8] S. E. Skipetrov, *Opt. Lett.* **28**, 646 (2003).
- [9] S. E. Skipetrov, *J. Opt. Soc. Am. B* **21**, 168 (2004).
- [10] T. Schwartz *et al.*, *Nature (London)* **446**, 52 (2007).
- [11] Y. Lahini *et al.*, *Phys. Rev. Lett.* **100**, 013906 (2008).
- [12] *Nonlinearity and Disorder: Theory and Applications*, edited by F. Abdullaev, O. Bang, M. P. Sørensen, NATO Science Series (Kluwer Academic Publishers, Dordrecht, 2001).
- [13] B. Liu, A. Yamilov, Y. Ling, J. Y. Xu, and H. Cao, *Phys. Rev. Lett.* **91**, 063903 (2003).
- [14] U. Bortolozzo, S. Residori, A. Petrosyan, and J. P. Huignard, *Opt. Commun.* **263**, 317 (2006).
- [15] H. De Raedt, A. Lagendijk, and P. de Vries, *Phys. Rev. Lett.* **62**, 47 (1989).
- [16] P. Sebbah, D. Sornette, and C. Vanneste, *Phys. Rev. B* **48**, 12506 (1993).
- [17] B. Ya. Zeldovich, N. F. Pilipetskii, A. V. Sukhov, and N. V. Tabiryan, *JETP Lett.* **31**, 263 (1980).
- [18] N. V. Tabiryan, A. V. Sukhov, and B. Zeldovich, *Mol. Cryst. Liq. Cryst.* **136**, 1 (1986).
- [19] I. C. Khoo, *Phys. Rep.* **471**, 221 (2009).
- [20] See supplemental material at <http://link.aps.org/supplemental/10.1103/PhysRevLett.106.103903> for a real time video of the speckle instability.
- [21] See, e.g., A. Buka and L. Kramer, *Pattern Formation in Liquid Crystals* (Springer-Verlag, New York, 1996), and references therein.
- [22] K. Busch, C. M. Soukoulis, and E. N. Economou, *Phys. Rev. B* **50**, 93 (1994).
- [23] Y. R. Shen, *The Principles of Nonlinear Optics* (John Wiley and Sons, Hoboken, NJ, 2003); G. Agrawal, *Nonlinear Fiber Optics* (Academic Press, San Diego, CA, 2007).
- [24] Y. Silberberg and I. Bar-Joseph, *J. Opt. Soc. Am. B* **1**, 662 (1984).
- [25] C. Vanneste and P. Sebbah, *Phys. Rev. Lett.* **87**, 183903 (2001).
- [26] A. Andreasen *et al.*, *Adv. Opt. Photon.* **3**, 88 (2011).